Technical Sciences
Academy of Romania
www.jesi.astr.ro

Journal of Engineering Sciences and Innovation
Volume 6, Issue 2 / 2021, pp. 159-174
http://doi.org/10.56958/jesi.2021.6.2.159

B. Chemical Engineering, Materials Science and Engineering

Received ***17 February 2021*** *Accepted* ***17 May 2021***
Received in revised from ***30 Apryl 2021***

Oxidative study of Acid Yellow 23 using K10-Montmorillonite chemically modified

DIANA-CARMEN MIRILĂ[*], DENISA-ILEANA NISTOR[*]

„Vasile Alecsandri" University of Bacău, Faculty of Engineering, Department of Chemical and Food Engineering, Laboratory of Catalysis and Microporous Materials, Mărășesti Bld., nr. 157, 600115, Bacău, Romania;

Abstract. Catalytic ozonation of the azo dye Acid Yellow 23 was investigated in the presence of Montmorillonite K10 and its chemically modified counterpart with Cobalt and Nickel (Co-Ni-K10). The material thus obtained were characterized by BET, XRD and TGA analysis. The effects of different variables were studied, such as: catalyst dose, ozone dose, ozonation time and pH. Clay-catalysed reactions are strongly dependent on the adsorption of the reactant, which in turn should depend on acid-base, electrostatic and hydrophilic-organophilic interactions. The basicity of the clay catalyst surface is expected to favour the interactions with the acidic groups of the studied organic molecule. The interactions involved in adsorption are determined by the pKa values of each group in each organic molecule.

Keywords: Advanced oxidation processes, ozonation, catalytic ozonation, K10 – Montmorillonite, azo dye, UV-Vis effects.

1. Introduction

Wastewater rich in organic dyes remains a major environmental problem. The presence of dyes in the environment has a negative impact on biodiversity and especially on aquatic fauna. This should impose stricter regulations for industrial producers that eliminate dye-rich wastewater [1]. Organic dyes are one of the largest groups of pollutants in wastewater released from the textile and food industry. Almost $7x10^5$ t and about 10000 different types of dyes and pigments produced annually worldwide are discharged into surface waters, and it is estimated that 1-15% of the dye is lost in effluents during the dyeing process [2]. Intensive industrial activities generate negative effects that are reflected by the degradation of the environment, affecting both the environment and human health,

[*]Correspondence addresses: miriladiana@ub.ro; dnistor@ub.ro

following their interaction with the resulting toxic effluents. The special interest dedicated to organic dyes results from their much higher concentration compared to a wide variety of organic pollutants released into wastewater from various industries (food, pharmaceutical, textile, etc.), hospital effluents and others [2-6]. Organic environmental dyes cause a major worldwide problem due to their acute and chronic toxicity. Dyes are widely used in large quantities in various industries, such as textiles, leather, food, cosmetics, paper, plastics, pharmaceuticals, etc. The textile industry alone accounts for two-thirds of total dye production [7]. The discharge of colored waste into streams affects their aesthetic nature and interferes with the transmission of sunlight into streams, reducing the photosynthetic action. Most dyes are toxic and very difficult to decompose, being a combination of chromophore groups such as nitroso (-N = O), nitro ($-NO_2$), azo (-N = N-) groups with aromatic rings and auxochrome fragments such as amino groups ($-NH_2$) and phenolic hydroxyl groups. This chemical structure determines not only the intensification of color, but also the chemical stability of aerobic biodegradation, light, heat and oxidizing agents. All oxidation techniques have a common feature, but have a disadvantage, namely the inevitable formation of harmful by-products. Oxidative treatments have been found to be essential for complete rehabilitation without any impact on biodiversity and human health. Compared to advanced oxidation processes, biological and physical water decontamination tests have proven to be unsatisfactory [8, 9]. Due to the large quantity and diversity of industrial textile dyes, the need to assess the impact of these dyes on the environment and especially on pollution has increased more and more. Dyes are slightly biodegradable, so conventional biological processes are not very effective in removing them [10].

One of the most important strategies for preventing water pollution is based on the retention of toxic effluents resulting from intense industrial activities on various adsorbents before they are released into the environment. The efficiency of the adsorption process depends largely on the properties of the adsorbent, the conditions of contact of the pollutant with the adsorbent particles, as well as the technological parameters. Due to the fact that the properties of the adsorbent decisively influence the efficiency of dye retention, it is necessary to prepare new materials that have a good regenerability, a high retention capacity and that are economically convenient. Research has shown a particular interest in the use of smectite clays as materials that can replace various adsorbents such as activated carbon for example in adsorption processes and advanced oxidation processes due to their availability in nature, good adsorption properties, such as and due to the very low cost of obtaining [11-13]. In order to fully mineralize dyes in different industries, the literature proposes the use of catalytic oxidation processes. These processes are sensitive to variations in: pH, temperature, ozone concentration, dye concentration, amount of catalyst and duration [14]. To combat these disadvantages of oxidation methods, this paper proposes the use of heterogeneous catalysts based on chemically modified cationic clays.

Experimental research carried out and presented in this paper, aimed to achieve clay-based materials in order to obtain new adsorbents / catalysts to be used in the adsorption / catalytic ozonation of AY23. The molecular structure of the dye is shown in (Fig. 1).

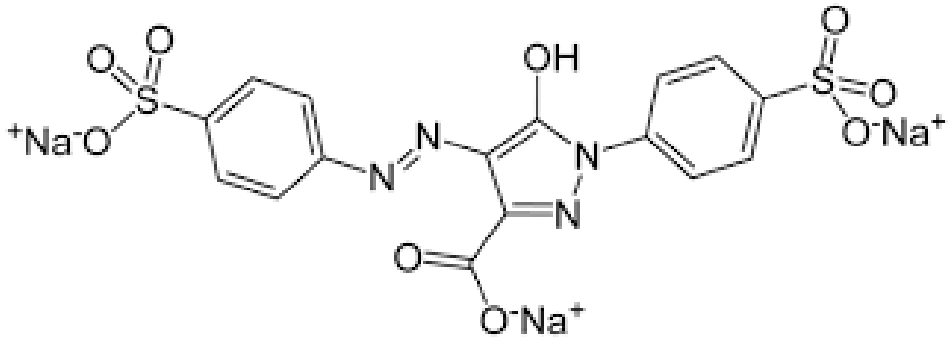

Fig. 1. Molecular structure of Acid Yellow 23 (AY23).

AY23 (E102) is an organic sodium salt, which is the trisodium salt of tartrazine acid. It acts as a histological dye and food dye, being one of the most stable, edible and synthetic pigments. It is widely used as a food additive, such as coloring in beverages (juice drinks, carbonated beverages), mixed beverages and confectionery. In addition, it has a wide range of uses in the pharmaceutical, cosmetics, clothing and other industries [3]. AY23 as an edible synthetic pigment, has the advantages of a strong coloration and a low price. Still, is on the list of carcinogens along with Blue Patent V (E131), Acid Red (E123), Food Green 4 (E142) and Sunset Yellow (E110). Food dyes, as seen on food labels, are found in considerable quantities, which can affect human health, causing various untreatable diseases.

2. Experimental

2.1. Materials and methods

All reagents used were purchased from Sigma Aldrich (NaOH, $AlCl_3$, $FeCl_2$, $CoCl_2$, $NiCl_2$ $AgNO_3$, Montmorillonite K10 (K10), AY23 ($C_{16}H_9N_4Na_3O_9S_2$), molecular mass: 534.36 g.mol^{-1}), Sunset Yellow FCF (SY-FCF, $C_{16}H_{10}N_2Na_2O_7S_2$), molecular mass: 452.37 g.mol^{-1}, Congo Red (CR, $C_{32}H_{22}N_6Na_2O_6S_2$), molecular mass: 696.665 g.mol^{-1}, Reactive Black 5 (RB5, $C_{26}H_{21}N_5Na_4O_{19}S_6$), molecular mass: 991.8 g.mol^{-1}, Methyl Orange (MO, $C_{14}H_{14}N_3NaO_3S$), molecular mass: 327.33 g.mol^{-1}, Evans Blue (EB, $C_{34}H_{24}N_6Na_4O_{14}S_4$), molecular mass: 960.81 g.mol^{-}1. Double distilled water was used throughout this work. AY23 were used as target molecule in aqueous solutions of 5 x 10^{-5} M concentration. For comparison, the raw material Montmorillonite K10 (Sigma-Aldrich) and its chemically modified counterpart with Fe-Al (AF-K10)[15] and Co-Ni (Co-Ni-K10) were used in the adsorption study. Decolourisation of dye was determined by measuring the

changes in the adsorbance at maximum visible adsorbance wavelength, which was recorded from the UV/VIS adsorption spectrum obtained from UV/Vis adsorption spectrophotometer BACKMAN DU 640. Dye decolourisation efficiency was determined as follows:

$$Rcolor(\%) = \frac{Abs\max, t0 - Abs\ max, t}{Abs\ max, t0} x\ 100 \quad (1)$$

Where: Ads max,t0 – initial adsorbance at at all characteristic peaks of dyes at reaction time 0, Ads max,t — adsorbance at at all characteristic peaks of dye at time t =30 s minimum and 300 s maximum;

2.2. Synthesis Co-Ni-K10

The synthesis of obtaining the Co-Ni-K10 adsorbent / catalyst was performed in two steps. In the first stage the homoionization of the initial material Montmorillonite K10 was performed by complete ion exchange, this was done three times. In a second step, the solution of 0.1 M $CoCl_2$ and 0.1 M $NiCl_2$ is added to each other dropwise at room temperature, under stirring. The obtained solution is added over the 2% K10 clay solution, at a temperature of 80 ˚C, for 4 hours, then it is polymerized for 10 minutes. The mixture is filtered with deionized water to remove excess Cl^- ions. The $AgNO_3$ test is performed to know if all Cl^- have been removed. The ionically exchanged clay thus prepared, is dried in steps (60, 80, 100 and 120 ˚C) for 1 h. The dry powder, named Co-Ni-K10, is calcined for 4 hours at 525 ˚C. Montmorillonite K10 was chosen as a raw material in the synthesis of adsorbents due to its high water dispersibility, low acidity and high Lewis basicity [16]. The synthesis of the adsorbent / catalyst (AF-K10) as well as its characterization, were published in a previous paper [15].

2.3. Characterization of Co-Ni-K10

BET analyses - Nitrogen adsorption-desorption analysis is frequently used to study the specific surfaces of nanocomposite systems. In addition, information on pore sizes and total pore volumes of nanomaterials is available using this analysis. In this area, (Fig. 2) shows the N_2 adsorption-desorption profiles for K10 and Co-Ni-K10. According to (Fig. 2) the isothermal shapes for all samples are closer to that of the IV isotherm, with H3 hysteresis loops in the desorption profiles. This type of isotherm is characteristic of micro / mesoporous materials.

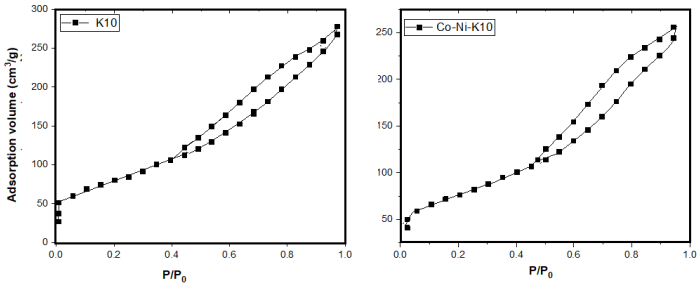

Fig. 2. N_2 adsorption–desorption isotherms of the (a) K10 and (b) Co-Ni-K10.

XRD analyses - both K10 and Co-Ni-K10 were characterized by X-ray powder diffraction using a Rigaku Geiger Flex diffractometer operating at 50 kV, 40 mA and aCuKα radiation (λ = 0.157 nm). As a common feature of homoionic montmorillonite, the complete ion exchange produced a sharp 001 XRD line and a shift of the basal distance d_{001} from 12 Å to 9 Å (Fig. 3), due to the compaction of the structure due to the removal of a large variety of larger sandwich species. Chemical modification of K10 with Co and Ni was supported by widening of the 001 XRD line (Fig. 3). After the modification of the clay material, the consecutive increase of the basal distance up to 12 Å to 26 Å indicates the formation of a large variety of sizes interspersed species[15].

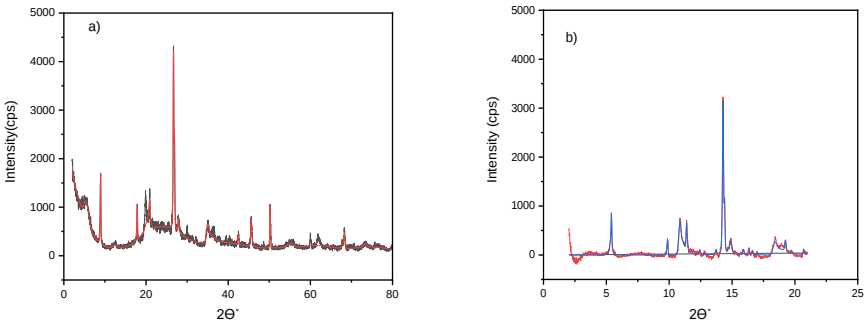

Fig. 3. XRD pattern a). K10 and b). Co-Ni-K10

TGA analyses -TGA and DTG curves of K10 intercalated with Ni (II) and Co (II) are shown in (Fig. 4). Thermal analysis of clay (K10) shows that the main weight losses (6%) occur at a temperature of 35 ° C to 280 ° C, which can be attributed to the loss of physically adsorbed water. The second mass loss (2%) in the range of 278 ° C to 580 ° C corresponds to the water loss that is related to the clay layers. The final weight loss is 2.50%, which is due to the loss of hydroxyl groups of the clay. The decomposition of the intercalated K10 compounds Ni (II) and Co (II) took place in three stages. In the first stage Ni (II) intercalated with K10, has a loss of mass (6.00%) from room temperature at 240 °C due to adsorbed water. The second stage of decomposition (5%), begins at 240 °C and ends at 720 ° C, is due

to the decomposition of the complexes that interspersed the clay layers. In the case of Co (II) intercalated with K10, the first step started at room temperature at 160 °C with a mass loss of 4%. The second stage shows a weight loss of 6% starting from 160 ° C to 500 °C. The weight loss in the third stage is 3% and 10% for Ni (II) and Co (II) intercalated K10, respectively. The residue for Ni (II) intercalated K10 and Co (II) intercalated K10 is approximately 86.00% and 80%, respectively.

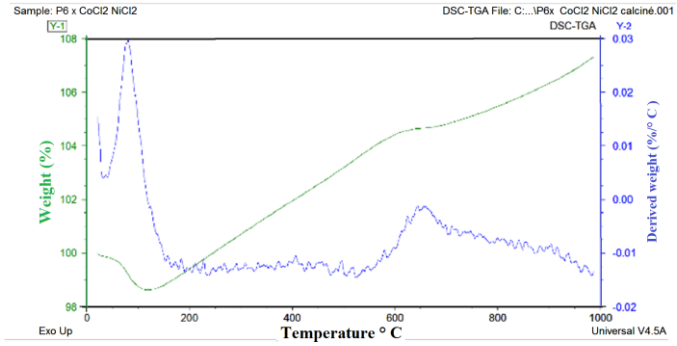

a)

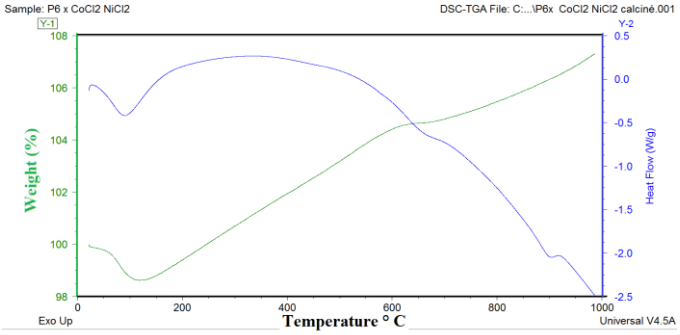

b)

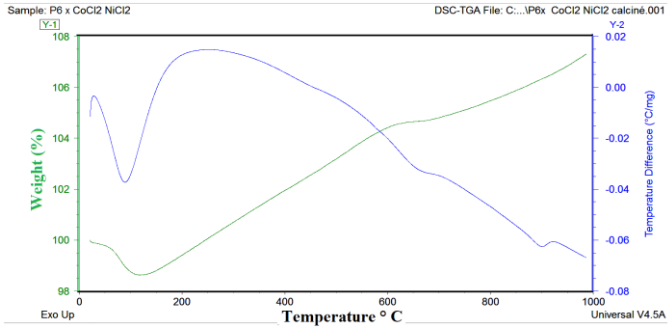

c)

Fig. 4. DSC-ATG Co-Ni-K10 analysis spectrum a). Derived weight; b). Heat flow; c). Temperature difference.

3. Results and discussions

During adsorption, simple ozonation as well as catalytic ozonation of the azo dye AY23 with 0.5, 1 and 1.5 gh^{-1} O_3, the location of the adsorption band in UV-VIS changes compared to a standard chosen as follows: by bathochrome displacement takes place a maximum adsorption to higher λ (nm) (and lower electronic transition energies ν) due to structural factors in the molecule of the organic compound; by hypsochromic displacement there is a shift of a maximum adsorption to lower λ (nm) (and higher electronic transition energies ν) due to structural factors present in the molecule of the tested organic dye compound and the increase or decrease of adsorption intensity is called hyperchromic effect or after case hypochromic. The effects are shown schematically in (Fig. 5).

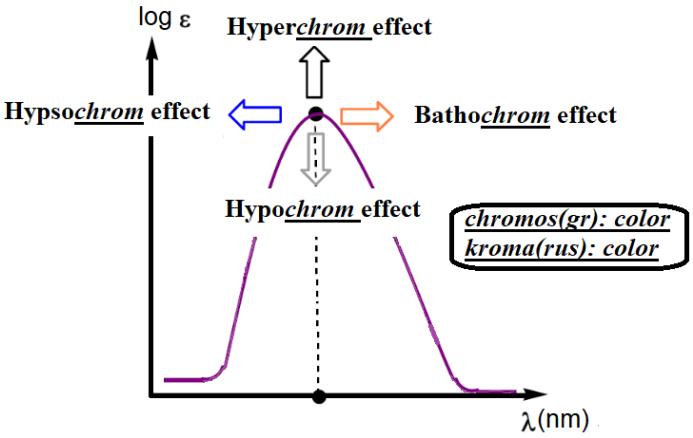

Fig. 5. Effects of displacement of an adsorption band in the U.V.-VIS

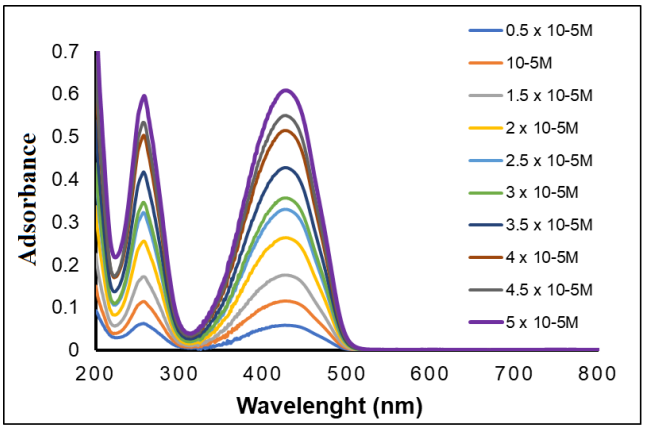

Fig. 6. UV-Vis calibration spectrum of non-ozonated AY23 at different concentrations (0.5 x 10-5 M - 5 x 10-5 M); distilled water (T = 22 ° C, 1 ml quartz cuve).

Table 1. The increase in adsorbance yield of AY23 on: K10, AF-K10 and Co-Ni-K10

Adsorbent	AY23 (E102) (425 nm) pKa 10.86			SY-FCF (E110) (482 nm) pKa 10.36 [17]			CR (497 nm) pKa 4.5 [18]		
	Adsorbent dose ($mg.L^{-1}$)	η (%)[b]	pH	Adsorbent dose ($mg.L^{-1}$)	η (%)[c]	pH	Adsorbent dose ($mg.L^{-1}$)	η (%)[d]	pH
K10	0	-	6.72	0	-	5.38	0	-	5.66
	2.5	11.48	5.43	2.5	13.90	5.43	2.5	8.20	5.87
	5	15.43	5.58	5.0	13.31	5.58	5	10.93	5.58
	10	24.65	5.65	10	33.91	5.65	10	14.75	5.40
	15	36.08	5.73	15	16.73	5.73	15	21.45	5.30
AF-K10	0	-	6.72	0	-	5.38	0	-	5.66
	2.5	4.32	9.31	2.5	5.03	9.31	2.5	10.60	7.65
	5	4.96	9.72	5.0	6.00	9.72	5	13.54	9.02
	10	10.01	9.62	10	10.18	9.62	10	20.69	9.43
	15	12.45	10.04	15	9.67	10.04	15	16.80	9.68
Co-Ni-K10	0	-	6.72	0	-	5.38	0	-	5.66
	2.5	7.86	6.12	2.5	6.01	5.61	2.5	3.88	5.94
	5	10.35	6.00	5	7.68	5.65	5	8.72	5.68
	10	13.5	5.88	10	14.65	5.65	10	13.56	5.70
	15	28.07	5.61	15	20.85	5.60	15	17.96	5.72

Table 1. The increase in adsorbance yield of AY23 on: K10, AF-K10 and Co-Ni-K10 (continuation).

Adsorbent	RB 5 (597 nm) pKa 10.16			MO (465 nm) pKa 3.4			EB (620 nm) -		
	Adsorbent dose ($mg.L^{-1}$)	η (%)[e]	pH	Adsorbent dose ($mg.L^{-1}$)	η (%)	pH	Adsorbent dose ($mg.L^{-1}$)	η (%)	pH
K10	0	-	5.86	0	-	5.49	0	-	5.89
	2.5	9.05	5.87	2.5	9.32	5.66	2.5	3.59	6.05
	5	12.27	5.80	5	13.25	5.47	5	6.28	5.30
	10	28.37	5.51	10	24.94	5.25	10	12.87	5.15
	15	47.85	5.60	15	29.53	5.19	15	14.75	5.07
AF-K10	0	-	5.86	0	-	5.49	0	-	5.89
	2.5	10.05	8.84	2.5	7.43	9.68	2.5	5.52	7.65
	5	14.77	9.16	5	13.93	9.80	5	4.82	8.66
	10	24.25	9.36	10	25.96	10.06	10	2.69	9.50
	15	36.84	9.85	15	41.60	10.30	15	3.41	9.60
Co-Ni-K10	0	-	5.86	0	-	5.49	0	-	5.89
	2.5	4.30	6.20	2.5	5.32	5.70	2.5	1.40	6.12
	5	14.28	5.95	5	10.35	5.86	5	5.15	5.50
	10	21.77	6.04	10	20.67	5.83	10	8.45	5.45
	15	31.12	5.88	15	23.62	5.68	15	13.17	5.41

The displacement efficiency of the dye adsorption on different adsorbents is presented in (Tab. 1). For comparison, in addition to AY23, five more azo dyes were used, namely: SY-FCF, CR, RB5, MO, EB. The best yields were obtained when using the adsorbent AF-K10 and Co-Ni-K10, which can be explained by a possible clay-dye synergy that involves adsorption by both hydrophobic interactions and additional acid-base interactions.

The dye calibration curve (Fig. 6) was plotted to evaluate the molar extinction coefficients (Tab. 2).

Table 2. Molar extinction coefficient (ε) for the different UV-Vis bands of AY23

Wavelenght (nm)		**Molar extinction coefficient (ε): ($L.mmol^{-1}.cm^{-1}$)***	**Correlation coefficient R^2**
AY23	425	24.574	0.9950
	256	24.102	0.9955

***** These coefficients were calculated from the slope of the linear part of the calibration curve fulfilling the Beer-Lambert's law.

3.1. Adsorption of AY23 on K10, AF-K10 and CO-Ni-K10

Dye adsorption was studied at a concentration of 5×10^{-5} M. Over 20 ml of dye solution were added different amounts of adsorbent: K10, AF-K10 and Co-Ni-K10 respectively (2.5, 5, 10, 15 mg). As expected, the general trend is not a progressive removal of dissolved dye molecules from the solution. This was supported by an increase in the adsorbance intensity over time at the characteristic wavelength (425 nm) for AY23 on K10 (Fig. 7a). In (Fig. 7b), when used as an adsorbent AF-K10, in addition to increasing the adsorbance to higher values (hyperchrome effect), there was also a shift to a shorter wavelength (hypsochrome effect) when was used 10 and 15 respectively mg of adsorbent. In (Fig. 7c) when the adsorbent Co-Ni-K10 was used, the same hyperchromic effect occurs as when using K10, except that the intensity of the increase in adsorbance is lower. In all three cases the increase in adsorbance was also supported by an intensification of the color of the dye solutions. Adsorption via acid–base interaction between AY23 (pKa 10.86) and acidic K10, AF-K10 and Co-Ni-K10 should not be involved. Besides, adsorption through cation exchange on catalysts, if any, should also have minor contribution.

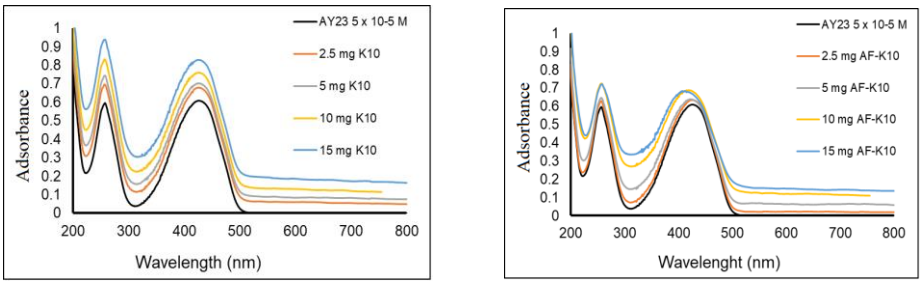

a) b)

Fig. 7. UV-Vis effects of AY23 solution ($5x10^{-5}$ M) on different adsorbent dose (2.5, 5, 10 and 15 mg), 20 mL of dye solution, a). K10 – hyperchromic effect; b). AF-K10- hyperchromic and hypsochromic effects; c). Co-Ni-K10- hyperchromic effect; contact time 30 s.

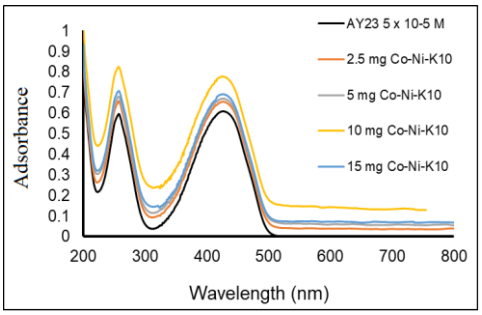

c)

Fig. 7. UV-Vis effects of AY23 solution ($5x10^{-5}$ M) on different adsorbent dose (2.5, 5, 10 and 15 mg), 20 mL of dye solution, a). K10 – hyperchromic effect; b). AF-K10- hyperchromic and hypsochromic effects; c). Co-Ni-K10- hyperchromic effect; contact time 30 s (continution).

3.2. Non-catalytic ozonation of AY23

The ozonation was performed in a 60 ml cylindrical glass reactor by bubbling ozone provided by an ozone generator (OZONFIX, Romania) using ambient air as inlet gas. Different series of ozonation tests were performed at 315 K. Periodic samples (10 ml) were taken at regular intervals, centrifuged to remove solid (2600 rpm) and analyzed by UV-Vis spectrophotometry (HELIOS OMEGA spectrophotometer, 1 cm quartz cuve). In (Fig.8.a), it is observed during the non-catalytic ozonation of the AY23 solution as the general trend, an increase of the adsorbance intensity at the characteristic wavelength of the food dye (425 nm) from the value 0.6077 to 0.6181 when is ozonated with 1.5 gh^{-1} O_3. When the solution is ozonated with a lower amount of O_3, respectively 0.5 gh^{-1}, a slight decrease in adsorbance from 0.6077 to 0.5959 is observed in the first 30 seconds, and this is probably due to improved ozonation for short reaction times without the production of small amounts of acidic species, an effect that is in accordance with a previously published paper[15]. This decrease is followed by the general tendency to increase the intensity after 60 seconds.

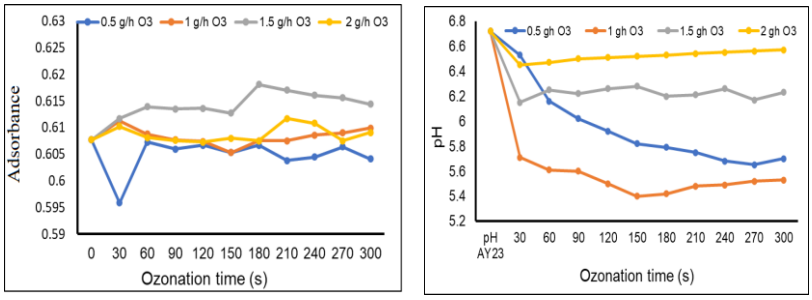

a) b)

Fig. 8. a). Non-catalytic ozonation of AY23 solution; b). Evolution in time of the pH during non-catalytic ozonation, at different O_3 throughputs in the absence of catalyst. Reaction mixture at intrinsic pH (starting value in the plot): 20 mL of dye solution.

It was found that the pH of the reaction mixture evolves differently over time depending on several variables, namely: dye molecule, ozone flow, absence / presence of ozone and type of catalyst. During non-catalytic ozonation, the general is a weak pH decrease in time from 6.72 to ca. 5.71 in the case of using 1gh^{-1} O_3 (Fig. 8.b).

3.3. Catalytic ozonation of AY23

Catalytic ozonation of the food coloring solution was performed with Montmorillonite K10 shown in (Fig. 9 a,b,c) and its chemically modified counterpart Co-Ni-K10 shown in (Fig. 10. a,b,c). As can be seen in (Fig.9) the general trend when adding the K10 catalyst is an increase in adsorbance in the first 30 seconds, followed by an approximately constant maintenance of up to 300 seconds of ozonation. As the ozone dose increases from 0.5 gh^{-1} to 1.5 gh^{-1} and the catalyst dose from 2.5 mg to 15 mg / 20 mL dye solution, the adsorbance value increases substantially from the initial adsorbance 0.6077 to approximately 0.9483, which is supported by (Fig. 7 a) due to the appearance of the hyperchrom effect.

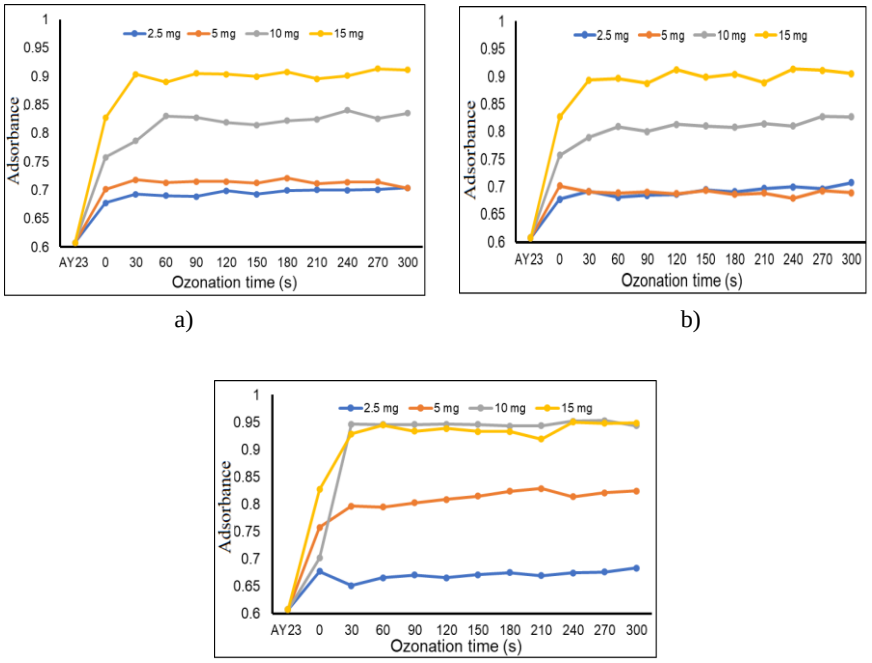

Fig. 9. Catalytic ozonation of AY23 solution (5x10^{-5}M, 20 mL), using a). 0.5 g.h^{-1} O_3; b). 1 gh^{-1} O_3; c). 1.5 gh^{-1} O_3 and different doses of K10 (2.5, 5, 10 and 15 mg), ozonation time (0 - 300 s).

Both during catalytic ozonation with K10 and its counterpart, the hyperchromic effect and the intensification of the solution coloration appear, respectively.

However, there is a difference in the adsorbance value, so that during ozonation with Co-Ni-K10 this value is lower by 0.0574, as can be seen by comparing (Fig. 9 c) with (Fig. 10 c).

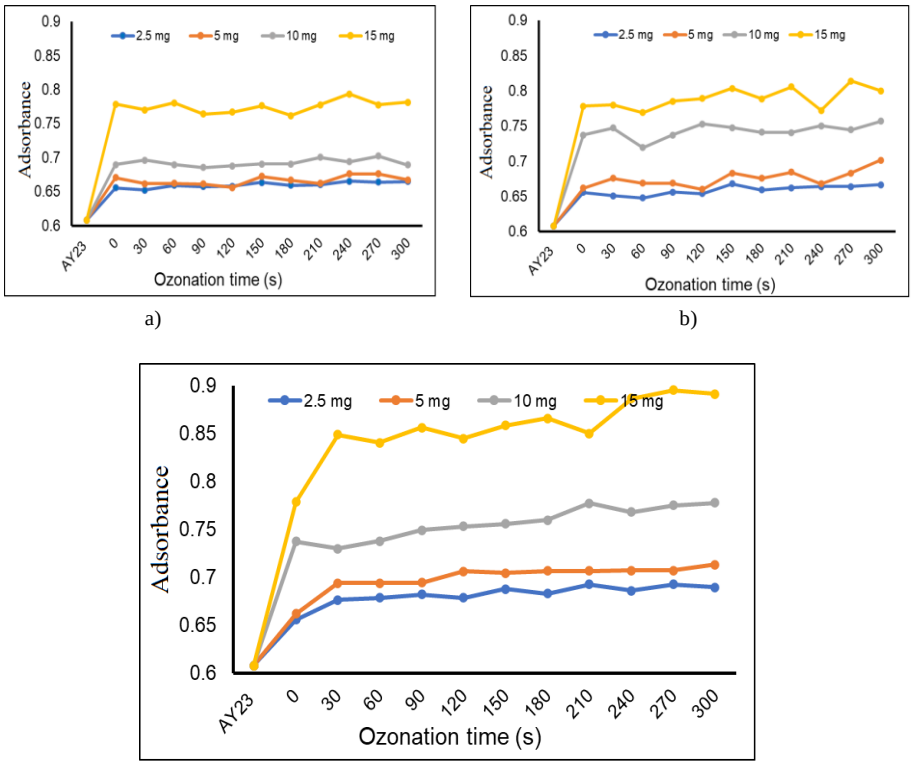

Fig. 10. Catalytic ozonation of AY23 solution ($5x10^{-5}$M), using a). 0.5 $g.h^{-1}$ O_3; b). 1 gh^{-1} O_3; c). 1.5 gh^{-1} O_3 and different doses of Co-Ni-K10 (2.5, 5, 10 and 15 mg), 20 mL of dye solution, ozonation time (0 - 300 s).

3.4. Evolution of pH during catalytic ozonation of AY23

The general trend of the pH of the AY23 solution when adding the K10 is a sudden decrease from the intrinsic pH of the food coloring solution 6.72 to cca. 5.91, a fact visible in (Fig. 11).

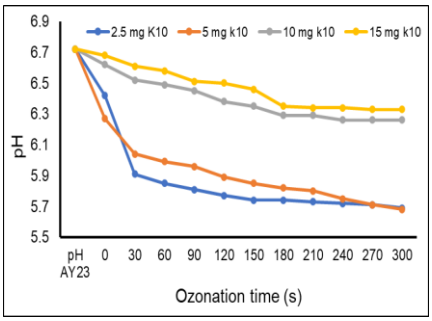

a)

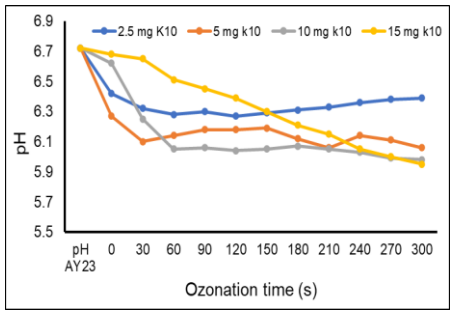

b)

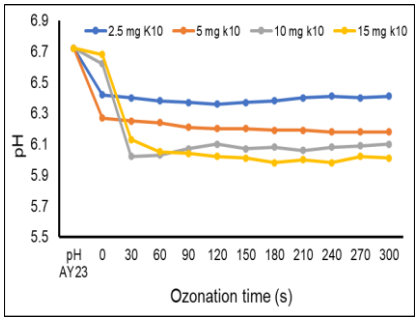

c)

Fig. 11. The evolution over time of the pH of the AY23 solution (20 mL) ozonated with a). 0.5 gh^{-1} O_3; b). 1 gh^{-1} O_3; c). 1.5 gh^{-1} O_3; for different doses of K10.

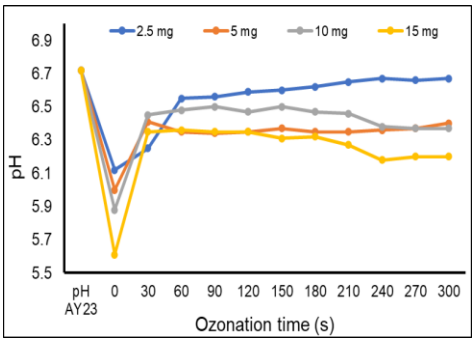

a)

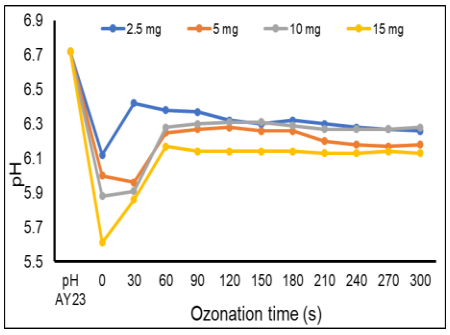

b)

Fig. 12. The evolution over time of the pH of the AY23 solution (20 mL) ozonated with a). 0.5 gh^{-1} O_3; b). 1 gh^{-1} O_3; c). 1.5 gh^{-1} O_3, for different doses of Co-Ni-K10.

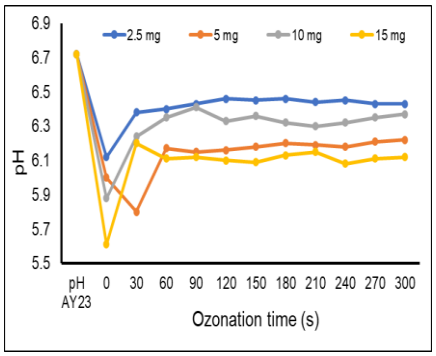

c)

Fig. 12. The evolution over time of the pH of the AY23 solution (20 mL) ozonated with a). 0.5 gh^{-1} O_3; b). 1 gh^{-1} O_3; c). 1.5 gh^{-1} O_3, for different doses of Co-Ni-K10 (continution).

In general, the presence of the catalyst leads in the first 30 seconds of ozonation using different doses of ozone, namely: 0.5, 1 and 1.5 gh^{-1}, to a sudden increase in pH over time, from 5.4 to approx. 6.45 (Fig.12). This increase in pH must be due to the appearance of amphoteric hydroxylated intermediates, in accordance with the literature[19, 20] and previous data [15].

4. Conclusions

Usually, in the first stage of ozonation, ozone dosage and catalyst concentration are undoubtedly the most important factors. In the case of adsorption as well as non-catalytic or catalytic ozonation of the azo AY23 food coloring solution, the mineralization did not take place due to the appearance of the hyperchromic and hypsochromic effects, providing clear confirmation of the nonoccurrence of dye adsorption / mineralization as can be noticed in (Table 1). The results were not as expected, the general trend was not a progressive removal of the dye molecule dissolved from the solution. This was supported by an increase in the intensity over time of the adsorbance of the AY23 solution (5 x 10^{-5} M) at 425 nm on all three catalysts K10, AF-K10 and Co-Ni-K10, and was also reflected by a visible progressive increase in solution coloration.

Acknowledgements: The authors are grateful to Mohamed Amine Didi for performing the BET, DRX and TGA analysis. No funding was provided for this study.

References

[1] E. Errais, *Réactivité de surface d'argiles naturelles: Etude de l'adsorption de colorants anioniques*, in, Strasbourg, 2011.
[2] I. Ali, V. Gupta, *Advances in water treatment by adsorption technology*, Nature protocols, **1**, 2006, p. 2661.

[3] V. Gupta, P. Carrott, M. Ribeiro Carrott, Suhas, *Low-cost adsorbents: growing approach to wastewater treatment—a review*, Critical Reviews in Environmental Science and Technology, **39,** 2009, p. 783-842.
[4] Y. Luo, W. Guo, H.H. Ngo, L.D. Nghiem, F.I. Hai, J. Zhang, S. Liang, X.C. Wang, *A review on the occurrence of micropollutants in the aquatic environment and their fate and removal during wastewater treatment*, Science of the total environment, 473, 2014, p. 619-641.
[5] D.C. Mirilă, M.Ș. Pîrvan, A.M. Roșu, V. Zichil, I.D. Nistor, *ACTIVATED ADSORPTION ON CLAY OF MICROPOLLUTANTS FROM PAPER PRINTING INDUSTRY*, Scientific Study & Research. Chemistry & Chemical Engineering, Biotechnology, Food Industry, 19, 2018, p. 63-72.
[6] I.M. Banat, P. Nigam, D. Singh, R. Marchant, *Microbial decolorization of textile-dyecontaining effluents: a review*, Bioresource technology, **58**, 1996, p. 217-227.
[7] P. Sharma, H. Kaur, M. Sharma, V. Sahore, *A review on applicability of naturally available adsorbents for the removal of hazardous dyes from aqueous waste*, Environmental monitoring and assessment, **183**, 2011, p. 151-195.
[8] L. Ren, G. Li, Y.C. Han, D.H. Jiang, H.-C. Huang, *Degradation of oxalic acid by Coniothyrium minitans and its effects on production and activity of β-1, 3-glucanase of this mycoparasite*, Biological Control, **43**, 2007, p. 1-11.
[9] M. Diez, *Biological aspects involved in the degradation of organic pollutants*, Journal of soil science and plant nutrition, **10**, 2010, p. 244-267.
[10] A.S. ALzaydien, *Adsorption of methylene blue from aqueous solution onto a low-cost natural Jordanian Tripoli*, American Journal of Applied Sciences, **6,** 2009, p. 1047.
[11] P.S. Nayak, B. Singh, Instrumental characterization of clay by XRF, XRD and FTIR, Bulletin of Materials Science, 30, 2007, p. 235-238.
[12] S. Babel, T.A. Kurniawan, *Low-cost adsorbents for heavy metals uptake from contaminated water: a review, Journal of hazardous materials*, **97**, 2003, p. 219-243.
[13] V. Gupta, *Application of low-cost adsorbents for dye removal–a review, Journal of environmental management*, **90**, 2009, p. 2313-2342.
[14] D.M. A. Azzouz, Ileana-Denisa Nistor, Farida Boudissa and R. Roy, *Advances in the oxidative degradation of organic pollutants: Prospects for catalyzed oxidation processes and targeting total mineralization*, J.C. Taylor (Ed.) Advances in Chemistry Research. , Nova Publisher, New York, 2019, p. 63.
[15] D.-C. Mirilă, F. Boudissa, A.-P. Beltrao-Nuñes, N. Platon, M.-A. Didi, I.-D. Nistor, R. Roy, A. Azzouz, *Organic Dye Ozonation Catalyzed by Chemically Modified Montmorillonite K10–Role of Surface Basicity and Hydrophilic Character*, Ozone, Science & Engineering, **42**, 2020, p. 517-530.
[16] A. Azzouz, A.-V. Ursu, D. Nistor, T. Sajin, E. Assaad, R. Roy, T*PD study of the reversible retention of carbon dioxide over montmorillonite intercalated with polyol dendrimers*, Thermochimica acta, 496, 2009, p. 45-49.
[17] M. Pérez-Urquiza, J. Beltrán, *Determination of the dissociation constants of sulfonated azo dyes by capillary zone electrophoresis and spectrophotometry methods*, Journal of Chromatography A, **917**, 2001, p. 331-336.
[18] N.B. Swan, M.A.A. Zaini, *Adsorption of malachite green and congo red dyes from water: recent progress and future outlook*, Ecological chemistry and engineering S, **26,** 2019, p. 119-132.
[19] S. Larouk, R. Ouargli, D. Shahidi, L. Olhund, T.C. Shiao, N. Chergui, T. Sehili, R. Roy, A. Azzouz, *Catalytic ozonation of Orange-G through highly interactive contributions of hematite and SBA-16–To better understand azo-dye oxidation in nature*, Chemosphere, **168**, 2017, p. 1648-1657.
[20] D. Shahidi, R. Roy, A. Azzouz, *Advances in catalytic oxidation of organic pollutants–Prospects for thorough mineralization by natural clay catalysts*, Applied Catalysis B: Environmental, **174,** 2015, p. 277-292.